Arctic Winter High Spectral Resolution Cloud Height Retrievals

Robert E. Holz* and Steven A. Ackerman
Cooperative Institute for Meteorological Satellite Studies,
Space Science and Engineering Center
University of Wisconsin-Madison
1225 W. Dayton St. Madison, WI, USA 53706-1612

Introduction

Developing accurate cloud climatologies of the Arctic has proven difficult. *In situ* observations are sparse and cannot provide the needed spatial distribution of cloud properties. Satellite measurements provide the needed spatial coverage, with frequent overpasses of polar orbiting satellites in the Arctic however, retrieving cloud properties from satellite measurements in the Arctic region is complex (Key et al., 1997).

The Atmospheric Infrared Sounder (AIRS) (Aumann et al., 2003), a polar orbiting hyperspectral radiometer capable of measuring infrared emission at very high spectral resolution offers an opportunity to improve the Arctic cloud retrievals. In this paper new Arctic cloud top retrievals, designed to extract the increased cloud information in the hyper spectral measurements, are developed with the goal of improving the Arctic winter cloud climatology.

There are significant differences in the Arctic environment compared to the lower latitudes that makes passive remote sensing difficult.

- Much of the Arctic surface is covered in snow or ice resulting in small thermal contrast between the surface and atmosphere
- There are persistent, strong surface temperature inversions
- During the Arctic winter there is no solar contribution
- Arctic clouds are often low and thin and composed of mixtures of ice and water (Curry et al., 1996)

Daytime Arctic detection of clouds is complicated by the reduced contrast between the snow-ice surface and clouds. For this reason reflectance tests using only visible channels do not have good sensitivity to clouds. To overcome the lack of contrast, near IR (1.6 μm) channels can be utilized. At these wavelengths clouds have larger reflectance compared to snow or ice. The increased reflectance results from the high sensitivity of cloud reflectance to particle size with higher reflectance for small particles sizes (Key et al., 1989). The ISCCP polar cloud detection algorithms use the 0.73 – 1.0 μm AVHRR channel to detect thin cirrus using these reflectance characteristics (Key and Barry, 1989).

The very cold surface temperatures, lack of sunlight, and strong surface temperature inversions make nighttime cloud retrievals even more difficult. The lack of sunlight prevents the use of reflectance measurements while the very cold surface temperatures and the frequent temperature inversions require different cloud detection methods compared the lower latitudes.

Hyperspectral Arctic Cloud Top Height Retrieval Development

The Arctic winter is characterized by frequent surface temperature inversions. In this paper a temperature inversion will be defined by its inversion strength and height where the height is defined as the maximum temperature in the atmospheric profile. If an isothermal layer exists at the inversion top, the top of the isothermal layer will be defined as the height. The inversion strength is defined as the temperature difference between the inversion top and the coldest layer between the surface and the top of the inversion. An example of a temperature and water vapor profile with a temperature inversion is presented in Figure 1. In this profile the inversion strength is approximately 11.0 degrees with an inversion height of 2.0 km.

Inversions can be detected by infrared measurements using spectral channels that have sensitivity to the lower atmosphere. If an inversion exists a channel with a weighting function that peaks near the inversion top will have an elevated BT relative to a profile without the inversion. For strong inversions the water vapor channel will be elevated relative to the window BT. This BT behavior was discovered using the High Resolution Infrared Sounder (HIRS) where it was found that over Polar Regions a negative BT difference occurred between 11 and 6.7 μm for FOV with strong surface inversions (Ackerman, 1996). The MODIS 7.2 μm channel is sensitive to water vapor in the lower atmosphere. The relatively high concentrations of water vapor in the low troposphere results in a strongly peaked 7.2 μm weighing function near the polar inversion top resulting in the elevated BT. Using this finding, a MODIS inversion

strength retrieval was developed (Liu and Key, 2003). This retrieval compares the MODIS 7.2 μm water vapor channel to the 11 μm window channel. The 7.2 μm channel weighing function peaks closer to the surface then the 6.7 μm channel improving the retrieval sensitivity for shallow or week inversions. An example of Arctic 7.2 μm and 6.7 μm channel weighting functions is presented in Figure 5. An empirical relationship between the BT differences and the actual inversion strength was developed using simulations allowing for retrievals of the actual inversion strength (Liu and Key, 2003). For temperature inversions less then 10 K the MODIS $BT_{7.3} - BT_{11}$ difference remains negative in Figure 4. For this reason a negative BT threshold is necessary to determine if an inversion exists. There is no single threshold that uniquely determines the existence of a temperature inversion, as this difference is dependent on the inversion strength, vertical depth of the inversion, and the concentration of water vapor. Using an optimal threshold it was found that 30% of the actual inversions were missed by MODIS and 7% were misidentified as inversions when an inversion did not exist (Liu and Key, 2003).

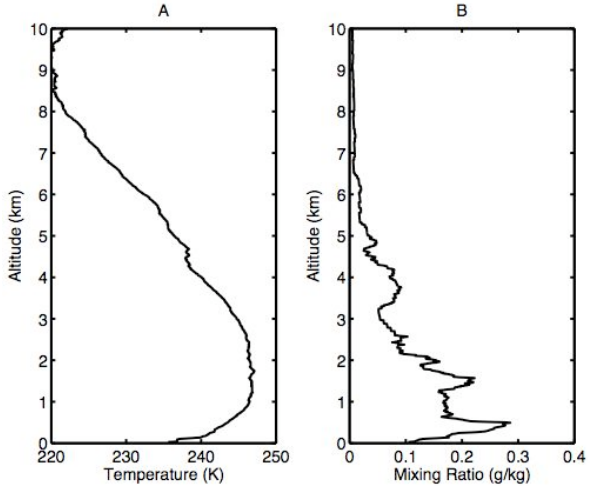

Figure 1: A Barrow NSA radiosonde profile is presented from February 8th 2004. Figure A is the temperature profile while figure B is the water vapor profile. Notice 12 deg inversion between 0 and 2 km and the low water vapor concentration.

In this paper a new hyperspectral inversion detection algorithm is presented that does not depend on a threshold to determine if an inversion exists. The hyperspectral measurements are able to resolve the water vapor absorption features between 1300 – 1500 wave-numbers in great detail. In the tropics and mid latitudes high concentrations of water vapor result in these channels being opaque to the surface. In the Arctic winter the atmosphere is extremely cold and dry allowing many of these channels to have sensitivity to the lower atmosphere. The hyperspectral measurements ability to resolve the water vapor absorption lines results in a large number of channels (>50) peaking throughout the lower atmosphere in the Arctic. This compares to only two channels for MODIS. The narrow weighting functions resulting from the higher spectral resolution increases the sensitivity to the Arctic temperature inversions.

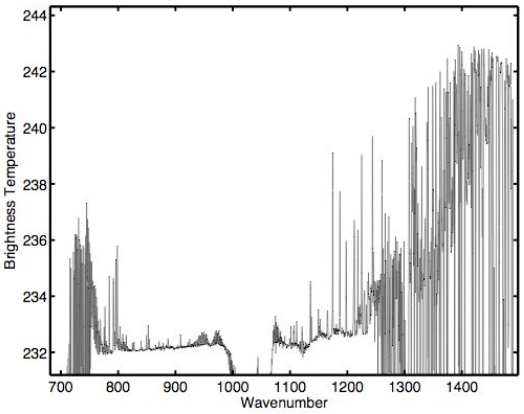

Figure 2: The simulated BT spectrum using the atmospheric profile in Figure 1. The inverted water and CO_2 lines are indicative of a strong inversion.

A clear sky simulation at the approximate resolution of AIRS was computed using LBLDIS for the temperature and water vapor profile in Figure 1. The results of the simulations are presented in Figure 2. In this spectrum the water vapor and carbon dioxide lines are inverted compared to a profile without a temperature inversion. This results in the water vapor channels (1300 – 1400 cm^{-1}) having a warmer BT compared to the 900 cm^{-1} window channels. In this spectrum the warmest channel is at 1393 cm^{-1}. The weighting function for this channel peaks at 2 km, the warmest temperature in the profile as presented in Figure 5. The weighting function for channel 1396, 1336, and the MODIS 6.7 and 7.3 μm bands are presented in the figure. The AIRS 1393 channel weighting function has significantly less sensitivity to the first 1.0 km of atmosphere compared to the MODIS 7.2 μm channel and a narrower peak resulting in an increased sensitivity to the inversion. The channel with maximum sensitivity to the inversion will vary depending on the height of the inversion and the distribution of atmospheric water vapor.

The hyperspectral inversion detection developed in this paper dynamically selects the water vapor channel by searching for the warmest channel in the spectral region

between 1200 – 1500 cm^{-1}. Selecting the warmest channel optimizes the sensitivity to the inversion, as the warmest channel will peak at the inversion top. This channel is then compared to the 960 cm^{-1} window channels. If an inversion is present that is detectable, the selected channel will have a BT warmer then the window channel. To reduce the sensitivity to noise at least 3 water vapor channels are required to be warmer then the window BT and the BT difference between warmest channel and the window BT needs to be greater then 0.2 K for a positive inversion determination.

Simulated AIRS clear sky BT spectra computed with varying inversion strengths is presented in Figure 3. The temperature profile used for the simulations was modified in the bottom 3 km so that the inversion top was located at 2 km. The difference between the inversion top and the surface was constrained to specified inversion strength. For increasing inversion strengths the water vapor lines between 1100 – 1400 cm^{-1} becomes increasingly warmer compared to the window channels. The relationship between the maximum BT water vapor channel and the 960 cm^{-1} window channel for varying inversion strengths is presented in Figure 4. The BT difference for the MODIS 6.7 μm and 7.3 μm vs. the 11μm channels is also presented. This figure illustrates the advantage of the hyperspectral retrieval compared to MODIS. As the actual inversion strength approaches zero the hyperspectral BT difference between the water vapor lines and the window BT converge to zero in contrast to the MODIS 6.7 μm and 7.3μm channel differences which become negative when the actual inversion strength is still approximately 10 K. The MODIS channel does not asymptote to zero but continues to decrease as the inversion strength becomes negative. Using the hyperspectral retrieval definitive inversion detection is possible. Based on these simulations inversion strengths of 2 K will result in BT difference of 0.5 K, above the noise threshold of AIRS. The sensitivity to the inversion strength is also dependent on the depth of the inversion and the lower atmospheric water vapor concentration. As a result the sensitivity will vary with the atmospheric conditions.

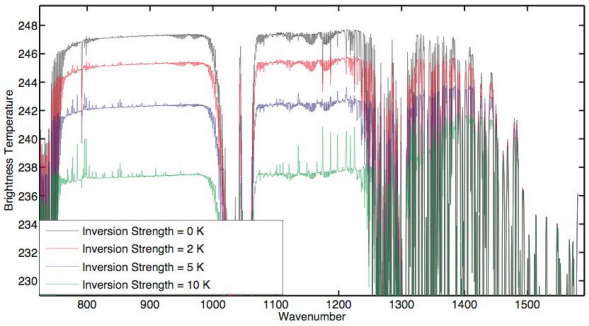

Figure 3: Simulated AIRS spectra for varying inversion strengths. The top of the inversion for the simulations was fixed at 2.0 km.

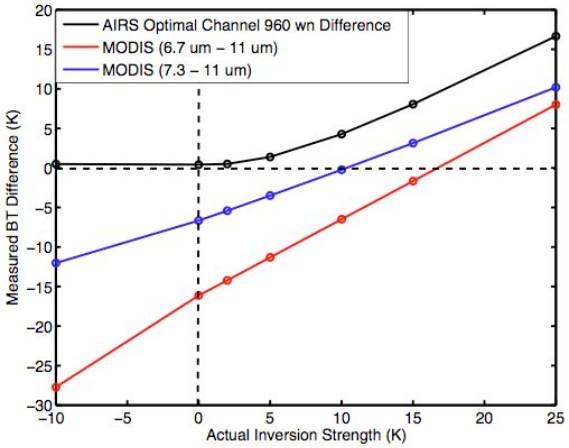

Figure 4: The simulated BT differences between the AIRS optimal channel selection and the 960 wavenumber window channel is compared to the MODIS 6.7 μm and 7.3 μm simulated window BT differences for varying inversion strengths. Positive inversion strength is one where the temperature increases with height from the inversion bottom. A negative value is one where the temperature decreases with height (no inversion) while a value of 0 is an isothermal atmosphere.

Arctic Stratus Hyperspectral Cloud Height Retrieval

The winter Arctic is a challenging environment to retrieve cloud top heights. A lower tropsophereic temperature inversion results in a non-unique window cloud top height if the cloud top temperature is between the inversion minimum and maximum temperatures. This problem is illustrated in Figure 6 and Figure 7 where the lidar measurements indicate a cloud top that resides in the strong but shallow inversion layer at approximately 1.2 km during the AIRS overpass at 22:02 UTC. An infrared

window cloud top retrieval can not retrieve a unique cloud top height because a cloud at both 1.2 km and 4.0 km results in the same measured window BT. Most operational cloud top retrievals will select the first matched window BT on the temperature profile. For this day this method would incorrectly retrieve a cloud height of 4.0 km resulting in a 3 km high bias.

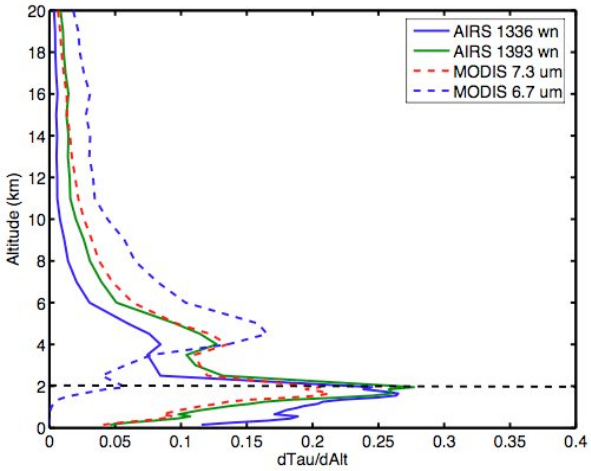

Figure 5: Channel weighting functions computed the radiosonde profile in Figure 1. Weighting functions for the MODIS 7.3 μm and 6.7 μm channels are presented as dashed curves. 2 AIRS channels are presented as solid lines. Notice the decreased width of the AIRS channels.

The ability of the hyperspectral measurements to uniquely determine the existence of a temperature inversion and the improved sensitivity to shallow inversions offers the opportunity to determine a unique cloud height for the cloud in Figure 6. A cloud located near the bottom of the inversion, as is the case on February 1st 2004 will enhance the measured inversion signature because the cloud top temperature is colder than the surface. A cloud above the inversion top will not show an inversion signature, as the cloud will block the inversion signal. The effect of the cloud heights on the measured BT spectra is presented in Figure 8. In this figure clouds below the inversion top have channels with warmer BT then the window channels. For clouds above the inversion top there is no inversion signature.

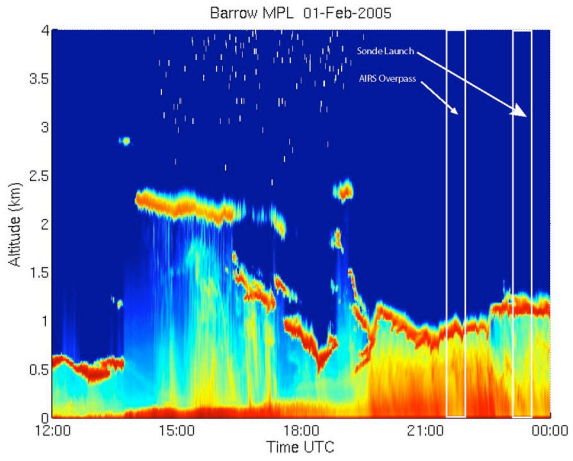

Figure 6: The MPL backscatter RTI image for February 1st 2005. There are low clouds with snow underneath between 12:00 – 2:00 UTC and 20:00 – 24:00 UTC. Between 14:00 – 16:00 UTC a there is a cloud at 2.5 km.

If a measured window BT of the cloud is between the inversion minimum and maximum temperature in the atmospheric profile the Arctic window cloud height retrieval uses the inversion to determine if an inversion is detected above the cloud. If an inversion is detected the Arctic cloud top retrieval matches the window BT to the profile below the inversion top. If an inversion is not detected the retrieval will match the measured window BT to the temperature profile above the inversion.

The impact of cloud optical depth on the cloudy inversion detection sensitivity was investigated using LBLDIS simulations with varying cloud optical thickness. The simulations used the atmospheric profile from the February 1st 2005 Arctic stratus case. The cloud boundaries measured by the lidar were between 1.1 – 1.2 km (Figure 6) at the 23:00 UTC, the time of the NSA radiosonde launch. Using the lidar boundaries a water cloud with an effective radius of 10 μm was simulated for different cloud optical thicknesses. The relationship between the cloud optical depth and the measured inversion strength is presented in Figure 9. The cloud optical depth is positively correlated with the inversion strength and as the cloud becomes opaque, the measured inversion strength asymptotes to 3.2 K. For optically thin clouds (OD < 1) the BT differences converge to the clear sky BT difference of 0.9 K.

The positive correlation between the cloud optical thickness and the measured inversion strength results from the relationship between the temperature structure of the atmospheric profile and the location of the cloud top. The magnitude of the measured inversion strength is

dependent on the difference between the temperatures of the background emission (the window channel) to the channels sensitive to the top of the inversion (the water vapor channels). In a clear atmosphere the window channel is sensitive to the surface emission. The cloudy atmospheric profile in Figure 7 has an elevated inversion with the inversion base near the cloud top altitude. In this profile the cloud top temperature is significantly colder than the surface temperature. As the cloud becomes optically thick the temperature contrast between the inversion top and the window channel increases as the cloud is colder than the surface temperature.

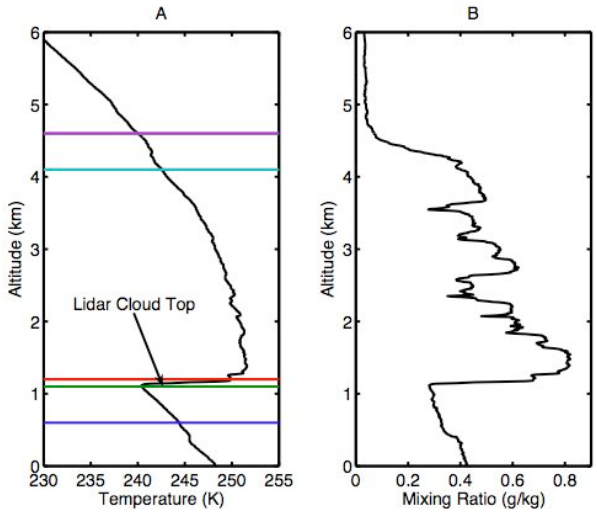

Figure 7: The temperature and water vapor profile at Barrow Alaska February 1st 2005. The lidar retrieved cloud top height is presented as the green line at 1.2 km. Notice the strong temperature depression near the cloud top altitude. The colored lines in figure A correspond to the cloud height used for each simulation presented in Figure 8.

The simulations predict a 3-degree BT difference between the window channel and the maximum water vapor channel. An AIRS overpass occurred at 22:02, one hour before the radiosonde launch. The measured AIRS BT spectrum for the overpass is presented in Figure 10. The AIRS measurements are consistent with simulations for a cloud below the inversion top as the water vapor channels between 1300 -1500 cm^{-1} are warmer than the window BT with a maximum difference of 2.14 K. A simulation with a cloud top at 1.2 km with an optical depth of approximately 2.0 is predicted to have a 2.3K. The total optical depth of the cloud at the AIRS overpass is less then 2.5 as the lidar is penetrating the cloud top. This is consistent with the simulations.

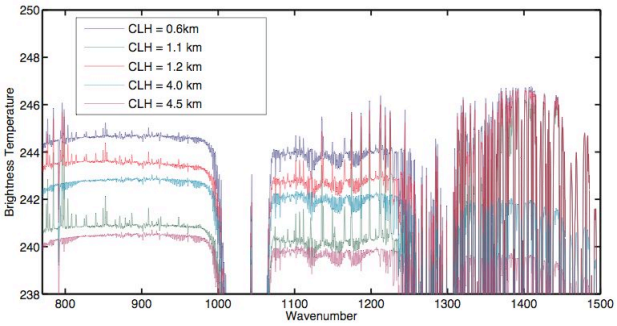

Figure 8: LBLDIS simulated cloudy spectra for varying cloud heights using the temperature and water vapor profile in Figure 7. The simulations used a water cloud with an optical depth of 10. The color of each profile corresponds to the colored lines on the temperature profile in Figure 7 (A) representing the cloud top height used in the simulations.

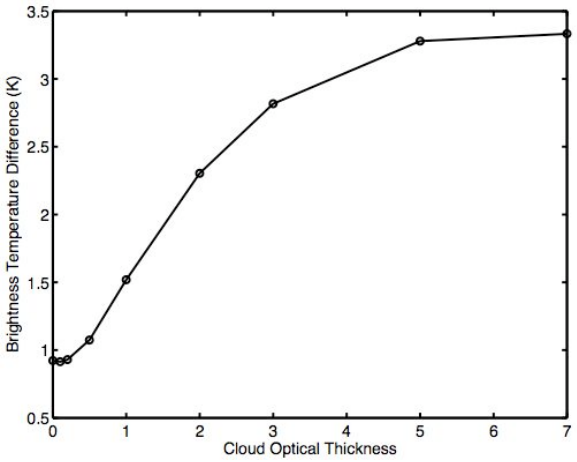

Figure 9: The relationship between the cloud optical thickness and the maximum water vapor channel BT compared to the 960 window BT is presented for February 1st 2005. The LBLDIS simulations used the NSA radiosonde profile presented in Figure 7 and a fixed cloud height of 1.2 km measured by the lidar. Only the cloud optical thickness was changed in the simulations.

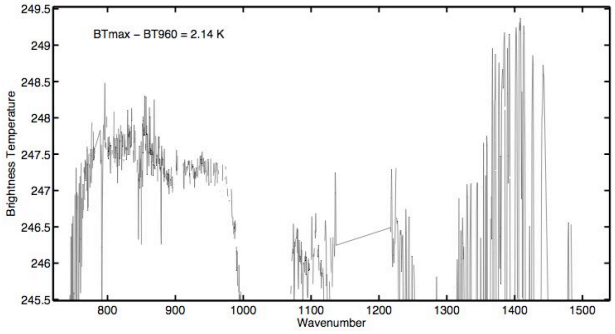

Figure 10: AIRS PCA filtered BT spectra at the NSA overpass at 22:02 UTC on February 1st 2005. The water vapor channels (1300 – 1450 cm $^{-1}$) are warmer then the window channels as predicted by the simulations for a cloud top below the inversion top. The maximum BT difference between the water vapor channels and the window is 2.14 K.

Hyperspectral Cloud Mask

The improvements to the MODIS Arctic cloud mask primarily a result of effectively using channels sensitive to the inversion top to determine the existence of an inversion in the measurements (Liu et al., 2004). This result suggests that the hyperspectral measurements should improve the cloud detection in the Arctic with the increased sensitivity to surface inversions. The hyperspectral retrieval is capable of uniquely identifying an inversion signature for inversion strengths as small as two degrees. MODIS requires significantly larger inversion strength to identify the inversion because of the broader spectral width. As part of the development of the hyperspectral cloud mask the method developed for the new MODIS Arctic cloud mask (Liu et al., 2004) was applied to the hyperspectral. It was expected that the significantly increased sensitivity of the hyperspectral measurements to the temperature inversions would improve on the MODIS results. However, a significant difficulty was encountered. The MODIS cloud mask assumes that if an inversion signature is present the FOV is clear. This is not the case for hyperspectral measurements. Using comparisons of AIRS FOV over the MPL at Barrow, AK found that AIRS detected inversions during 44% of the all the AIRS cloudy FOV as determined by the MPL over a three month period of AIRS overpasses. No significant correlation between the measured AIRS inversion strength and the cloud height was found as presented in Figure 11. This finding suggests that a detected inversion in the hyperspectral measurements provides little information about clouds in the AIRS FOV. This is a surprising finding as the MODIS $BT_{7.2} - BT_{11}$ test used in the MODIS Arctic cloud mask demonstrates significant skill at distinguishing clouds from clear even though both techniques use similar channels sensitive to lower atmospheric inversions. Figure 11 offers a clue to why a detected inversion in the hyperspectral does not demonstrate skill at discriminating clear from clouds. The maximum inversion detected by AIRS when the ARM MPL determined the FOV cloudy was approximately 9.0 K. When AIRS measured inversions greater then 9 K the NSA site was clear based on the MPL. The increased inversion sensitivity of AIRS compared to MODIS presented Figure 4 suggests that the MODIS $BT_{7.2} - BT_{11}$ difference becomes positive when the measured AIRS inversion strength is greater then 5 K. The lower inversion sensitivity of MODIS results in MODIS missing the weaker inversion for cases where AIRS detected the inversion above the cloud. The results suggest that it can be cloudy when MODIS detects an inversion and that the MODIS cloud mask should not depend just on the inversion detection to determine clear from cloudy.

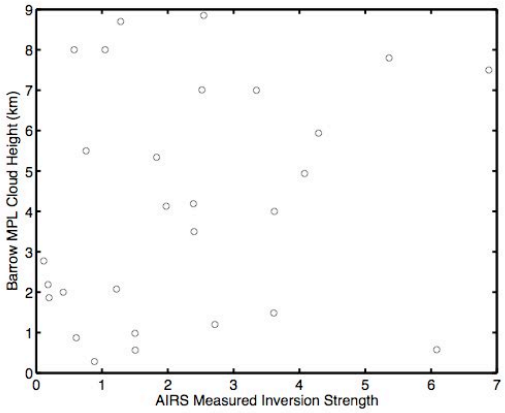

Figure 11: The AIRS measured inversion strength is compared to the cloud height measured by the MPL at the Barrow NSA facility. In this comparison 44 % of the ARCL detected cloudy FOV had an AIRS detected inversion.

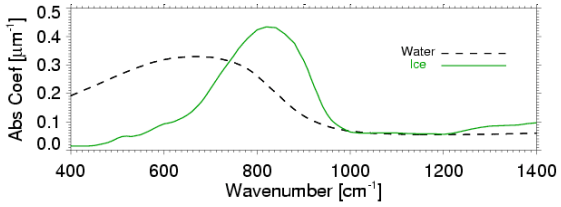

Figure 12: The absorption coefficient for ice and water for infrared wavelengths. Significant differences between ice and water occur between 400 – 1000 wavenumbers.

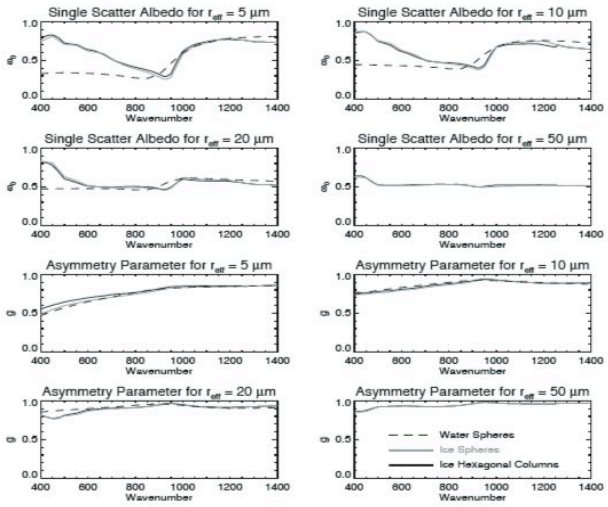

Figure 13: The single scatter albedo and asymmetry paremater for ice and water for 5,10,20 and 50 µm effective radius spheres (Turner, 2003).

The maximum temperature inversion measured by AIRS when clouds were detected by the MPL was approximately 9.0 degrees. This suggests that if AIRS measures an inversion greater then 10 K the FOV is probability clear however this is based on a limited data set in one location in the Arctic. More information is needed to uniquely determine clear from cloudy.

Spectral differences between clouds and the Arctic surface offer another means to determine if a FOV is cloudy. If the spectral characteristic of the surface is different than clouds these differences can be used to improve the cloud mask. The differentiation between ice and water clouds has been demonstrated using the spectral differences between 8 – 13 µm (Ackerman et al., 1990: Baum et al., 2000: Strabala et al., 1994). The BT difference results from a combination of the different imaginary index of refraction between ice and water, the different size and shape of ice crystals compared to water, and difference in the cloud heights with ice clouds typically higher then water clouds.

The absorption coefficient is dependent on the imaginary index of refraction related by:

$$k = \frac{4\pi m_i}{\lambda}$$

Where k is the absorption coefficient, m_i is the imaginary index of refraction, and λ is the wavelength. The absorption coefficient computed using m_i for ice and water is presented in Figure 12. There are significant differences between ice and water between 800 – 1000 cm^{-1} with ice having a higher absorption coefficient compared to water at 800 cm^{-1}. Above 1000 cm^{-1} the absorption coefficients do not have significant variation. Clouds with similar microphysical characterizes except for the phase will result in the ice cloud having a warmer measured BT compared to water at 800 cm^{-1}. Above 1000 cm^{-1} ice and water will have the same measured BT as the index of refraction between ice and water is very similar at these wavelengths. The difference in the absorption coefficient at 800 cm^{-1} and not at 1100 cm^{-1} contributes to the different spectral characteristics between ice and water.

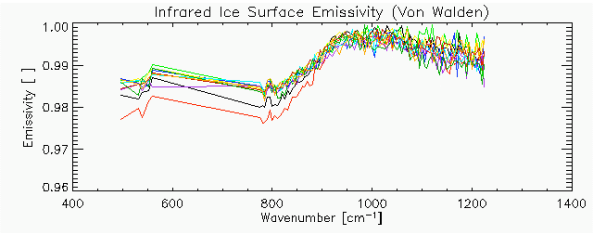

Figure 14: The measure spectral resolved emissivity of an ice surface is presented. Down looking Atmospheric Emitted Radiance Interferometer (AERI) measurements where used to retrieve the surface emissivity (Mahesh et al., 2001).

The different spectral characteristics between ice and water are not only influenced by the differences in m_i, but also the effective radius of the cloud, as the single scatter albedo is strongly dependent on the particle or drop size. The relationship between ice and water for different R_{eff} is presented in Figure 13. Ice cloud effective radiuses are typically larger than water clouds. From Figure 13 the single scatter albedo is significantly smaller at 800 cm^{-1} compared to 1100 cm^{-1} for small particle sizes (reff < 20). As the particle size increases the change in single scatter albedo with wavelength is reduced.

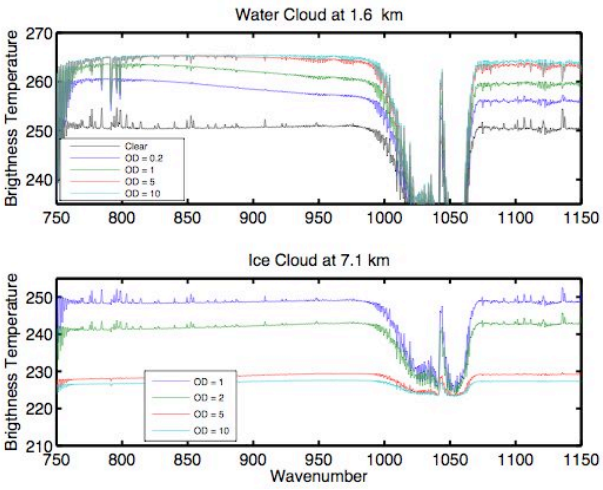

Figure 15: Simulated BT spectra for ice and water using the NSA atmospheric profile from January 1st 2004. The upper plot used a cloud composed of water spheres at 1.6 km while the lower plot was simulated using ice spheres at 7.1 km. Only the cloud optical depth was modified.

The cloud height also influences the measured spectra between 800 – 1100 cm^{-1} as the concentration of water vapor is strongly dependent on altitude. Ice clouds are typical in the upper troposphere where there is a significantly lower water vapor concentration. For low clouds the water vapor above the cloud acts to suppress the 1100 cm^{-1} channels due to the increased water vapor absorption at 1100 cm^{-1}.

The measured spectral emissivity of an ice surface is presented in Figure 14. Down looking Atmospheric Emitted Radiance Interferometer (AERI) measurements of the Antarctic surface were used to retrieve the surface emissivity (Mahesh et al., 2001). The ice surface emissivity has spectral dependence between 800 - 1100 cm^{-1} with an emissivity of 0.985 at 800 cm^{-1} compared to 0.995 at 1100 cm^{-1}. A one percent change in surface emissivity results in a 2.5-degree temperature difference at 250 K. If differences between the surface and cloud spectral emissivity exist, and are large enough to be resolved in the hyperspectral measurements these differences could be used to determine clouds from clear.

The upwelling radiance measured by a satellite is dependent on both the cloud, atmosphere, and surface spectral properties discussed in this chapter. To investigate the radiance difference between cloudy and clear FOV radiative transfer simulations using LBLDIS for both ice and water clouds with varying optical depth and effective radius were simulated. The ice simulations used Mie scattering properties for both ice and water clouds. The AERI surface emissivity measurements presented in Figure 14 were used for the surface properties in the simulations. The results from these simulations are presented in Figure 15. The computations used an NSA radiosonde profile from January 1st 2004. The slope of the BT spectra for a water cloud at 1.6 km between 800 and 960 cm^{-1} is small for cloud optical depths greater then 5.0. Optically thin water clouds (OD <4) have a negative slope in the BT between 800 – 960 cm^{-1}. For the ice cloud at 7.1 km the slope of the spectra between 800 – 960 cm^{-1} is positive. As the optical depth increases the slope of the spectra decreases.

The BT difference between 800 and 1100 and 960 - 1100 cm^{-1} micro-windows is presented in Figure 16 for a range of cloud optical depths and R_{eff} for both water and ice clouds. The simulations demonstrate that there is a significant BT difference between ice and water between BT800 – BT1100 with water clouds having a positive BT800 – BT1100 difference compared to the negative differences for the ice cloud. An important finding for the development of the hyperspectral cloud mask is that for both ice and water clouds the AIRS BT800 – BT1100 differences were significantly different from the clear sky simulations. The simulated differences where greater then 0.5 K except for ice clouds with large R_{eff} and small optical depths. As most ice clouds have R_{eff} smaller than 40 μm the simulations results suggest that the BT800 – BT1100 channel difference can be used to distinguish ice clouds from the Arctic surface. For water clouds the largest BT differences are for optically thin clouds (OD < 3). For optical depths greater then 3 the droplet R_{eff} has a reduced impact on the measured BT difference. The smallest BT800 – BT1100 differences occur at large water cloud optical depths with the BT differences of 1.8 K for a cloud optical depth of 10. For all cases simulated, the BT800 – BT1100 differences were significantly different than the clear sky BT800 – BT1100 differences. The BT960 – BT1100 cloudy channel difference has less contrast compared to the surface with differences of about 1.0 degree.

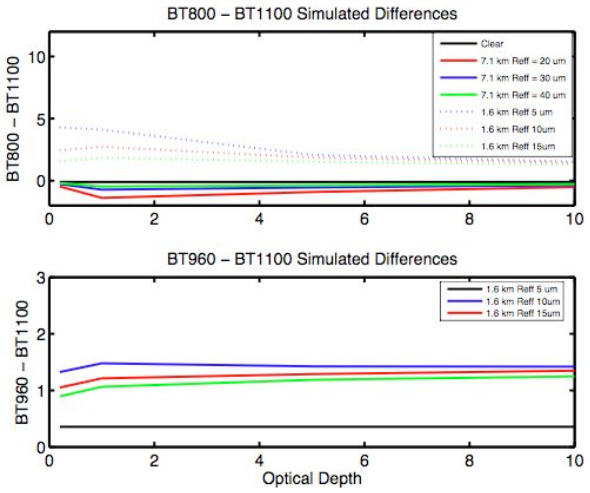

Figure 16: The Brightness Temperature (BT) difference between the 800 – 1100 and 960 -1100 channels with changing cloud optical depth and cloud effective radius is presented for both water and ice clouds. The Clear sky difference between the channels is presented as a black line.

A Optimal Cloud Height Retrieval

The simulations presented in this paper are promising for developing a spectrally based hyperspectral cloud mask. They demonstrate that the BT800 – BT1100 differences contain information about the cloud phase. This technique has been successfully demonstrated using MODIS measurements (Baum et al., 2000: Strabala et al., 1994). The cloudy BT800 -BT1100 differences compared to the clear sky suggest that this channel pair has information about the presence of clouds in the FOV. The clear sky BT800 – BT1100 difference in the simulations was -0.10 K. For both the water and ice cloud the contrast between clouds and clear was greater than 0.2 K except for optically thin ice clouds with large R_{eff}.

Comparisons with the ARM measurements at the NSA found that for AIRS inversion strengths greater the 9 K clouds were not detected by the MPL. Using this finding, if the AIRS measured inversion strength is greater then 10 K, the FOV is determined clear. For inversions strengths less then 10 K the AIRS BT800 – BT1100 difference is used to determine if the FOV is clear or cloudy. The tests used in the hyperspectral cloud mask are presented in Table 1.

Table 1: Cloud Mask Spectral Tests

Cloud Mask Test	Thresholds
Measured Inversion Strength	> 10 K → Clear
BT800 – BT1100	< -0.05 → Ice cloud (CO_2 Slicing) > 1.0 → Water cloud (Arctic Window)
BT960 – BT1100	> 1.0 K → Water cloud (Arctic Window)

The cloud mask first checks the retrieved inversion strength in the FOV. If the inversion strength is greater then 10 K the FOV is determined clear. The 10-degree threshold was determined using a comparison of 150 AIRS FOV over the NSA site. If an inversion is detected but the inversion strength is less then 10 K the BT800 – BT1100 and BT960 –BT1100 differences are used to determine if the FOV is cloudy. As demonstrated by simulations in Chapter 0 the BT800 - BT1100 difference will be positive and greater than 1.0 K for most water clouds while ice clouds will have BT differences less than - 0.1 K. If the BT800 – BT1100 difference is greater the 1.0 K or less then -0.05 K the FOV is determined cloudy. The BT960 – BT1100 differences demonstrated less surface contrast compared to the BT900 – BT1100 channel differences. Experimentation with real AIRS measurements found that the addition of this channel difference improves the cloud determination. The reduced water cloud R_{eff} sensitivity of the BT960 – BT1100 differences may contribute to the improvement. Based on the simulations and experimentation with real AIRS measurements if the BT960 – BT1100 channel difference is larger then 1.0 K the FOV is determined cloudy.

If an FOV is determined cloudy a method to select the optimal cloud height retrieval (CO2 Sorting/Slicing or the Arctic Window retrieval) is needed. The optimal cloud height retrieval depends primarily on the cloud height. The CO_2 Sorting/Slicing retrieval is most accurate for optically thin, upper tropospheric clouds while the Arctic window retrieval is optimized for low Arctic stratus. High clouds (above 5 km) are primarily composed of ice due the very cold Arctic temperatures. Using this observation the BT800 – BT1100 high sensitivity to ice can be used to select between the

Sorting/Slicing and Arctic window retrieval. BT800 – BT1100 differences less the 0 K are correlated with the presence of an ice cloud. Using this information if the BT800 –BT1100 difference is less then -0.05 K the hyperspectral cloud retrieval selects the CO_2 Sorting/Slicing retrieval as the optimal cloud height. For BT800 – BT1100 differences greater then 1.0 K or BT960 – BT1100 greater then 1.0 K the Arctic window cloud height retrieval is selected. FOV with the BT800 – BT1100 difference between -0.1 K and 1.0 K and BT960 – BT1100 differences less then 0.9 K determined clear.

Validation

The AIRS hyperspectral cloud top retrievals are compared to coincident ground and aircraft measurements over the North Slope of Alaska (NSA). The accuracy of the Arctic window cloud top retrieval and the CO_2 Sorting/Slicing retrieval in Arctic conditions is investigated. The validation consists of comparisons of individual AIRS granules to the ground and aircraft measurements.

Mixed Phase Arctic Cloud Experiment (MPACE)

The Mixed Phase Arctic Cloud Experiment (MPACE) funded by the Department of Energy Atmospheric Radiation Measurement (ARM) program during September and October 2004 provided a unique validation data set to investigate the AIRS hyperspectral cloud top height retrievals. During MPACE extensive aircraft and ground measurements was collected along the North Slope of Alaska (NSA) with frequent over flights of the ARM NSA ground facility. The AHSRL was operated during MPACE at the ARM NSA site at Barrow providing well calibrated vertically resolved extinction and depolarization measurements. Two aircraft platforms, the Scaled Composites Proteus and the University of North Dakota Cessna Citation aircraft provided both high altitude and *in situ* measurements of the cloud microphysical and radiative properties. The S-HIS and the Cloud Detection Lidar (CDL), a single channel lidar capable of cloud boundary detection flew on the Proteus. The Citation flew with extensive *in situ* instruments capable of measuring the cloud microphysical properties. This section will investigate MPACE measurements focusing on days when aircraft measurements where available over NSA.

October 17th 2004

High Cirrus clouds where present over the NSA site on October 17th 2004 as presented in Figure 18. An AIRS overpass of the NSA site occurred at 22:22 UTC. As determined by the AHSRL aerosol backscatter cross-section in Figure 18 the cloud boundaries where between 4.5–10 km. The cloud is composed of ice as the AHSRL measured depolarization is above 25%. The Proteus was coordinated with the AIRS overpass providing down looking Lidar (CDL) cloud boundaries in Figure 17 with a measured cloud top at approximately 10 km. The results of the AIRS optimal hyperspectral cloud top retrieval for the AIRS overpass at 22:20 UTC is presented in Figure 19. The Barrow NSA site is marked as the green dot in the figure while the black line is the flight track of the CDL. The results of the cloud mask are presented in Figure 22. For the FOV over the Barrow NSA site the cloud mask selected the hybrid Sorting/Slicing retrieval. The mask determines the retrieval method using spectral tests. The Sorting/Slicing retrieval is selected if the BT spectra has an ice signature as determined by the BT800 – BT1100 cm^{-1} channel differences. For FOV with differences less then - 0.05 K the CO2 Sorting/Slicing retrieval is selected. The BT800 – BT1100 differences for the AIRS NSA overpass are negative over NSA as presented in Figure 23. This is in agreement with the high depolarization measured by the AHSRL in Figure 18. It is encouraging that the BT800 – BT1100 channel difference correctly selected the CO2 Sorting/Slicing retrieval presented in Figure 19.

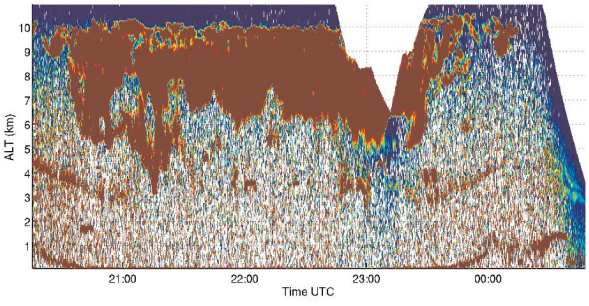

Figure 17: The Cloud Detection Lidar backscatter profile on October 17th 2004. The CDL was onboard the Proteus aircraft. The flight track of the Proteus is overlaid on Figure 19. The Proteus flew over the Barrow NSA ground facility multiple times between 22:00 – 23:30 UTC. The Proteus descended into the cloud between 22:40 – 23:20 UTC explaining the lack of data between 7 -11 km during this period.

The coincident MODIS Aqua cloud top pressure retrieval for the overpass is presented in Figure 21. MODIS retrieves the high cirrus over the NSA site however there is considerably more variability in the cloud heights compared to the AIRS retrievals. The CDL backscatter profile in Figure 17 retrieves a constant 10 km cloud top height during the flight. The AIRS retrieved cloud emissivity is presented in Figure 20. The optically thick region of the cloud is located just to the west of Barrow and extends to the north and south. The AIRS CO_2 Sorting/Slicing cloud top height demonstrates little

cloud top height variability, constant with the CDL, while retrieving significant cloud emissivity variability. The MODIS cloud top pressure is tends to correlate with the AIRS cloud emissivity with the MODIS cloud heights highest where the AIRS cloud emissivity is large. This variability is likely not real as the CDL does not show significant cloud top height over this region. Instead this variability is likely caused by errors in the MODIS CO_2 slicing retrieval. The CO_2 Sorting/Slicing is designed to be less sensitive to errors in the surface characteristics and lower atmospheric temperature profile. It is encouraging that the AIRS cloud height variability is consistent with the lidar.

The AIRS optimal cloud top retrieval in Figure 19 retrieved low clouds south east of Barrow. The cloud mask selected the Arctic window retrieval and retrieved a cloud height of approximately 4 km. Close inspection of the CDL lidar backscatter reveals a cloud under the cirrus with a varying cloud tops between 3-5 km in Figure 17. The optical thickness of the cirrus is likely less then 2.5 as the CDL maximum optical depth sensitivity is less then 2.5 and the lidar is penetrating the cirrus. The cirrus optical depths in this region are likely below the sensitivity of AIRS resulting the 4 km retrieval of the thicker clouds below the cirrus in the CDL profile.

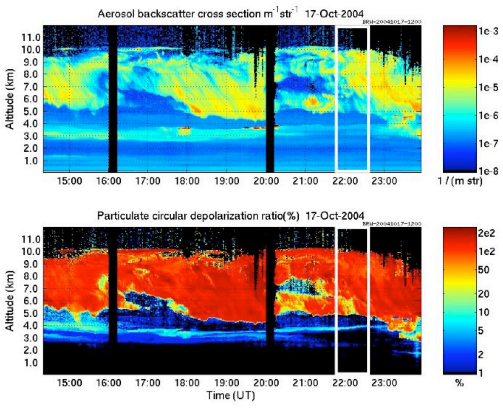

Figure 18: The AHSRL Aerosol backscatter cross-section and depolarization is presented for October 17th 2004. The HSRL was located at the Barrow NSA site marked by the green dot in Figure 19. The high depolarization between 5 -10 km is indicative of an ice. An AIRS overpass occurred at 22:22 UTC. The white box in the figure marks the time period of the AIRS overpass.

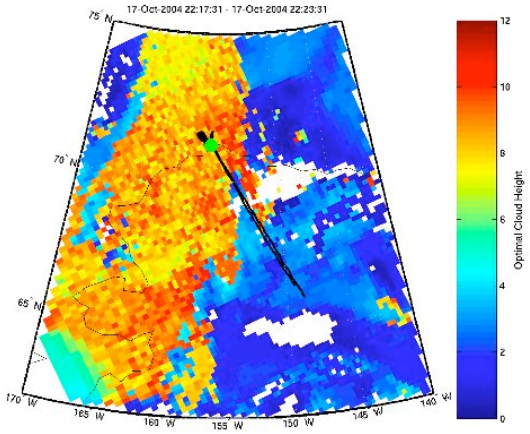

Figure 19: The AIRS hyperspectral optimal cloud height retrieval for the October 17th 223 granule between 22:17 – 22:24 UTC. The Barrow NSA research facility is marked by the green dot in the figure. The flight track of the Proteus is overlaid as the black line on the figure.

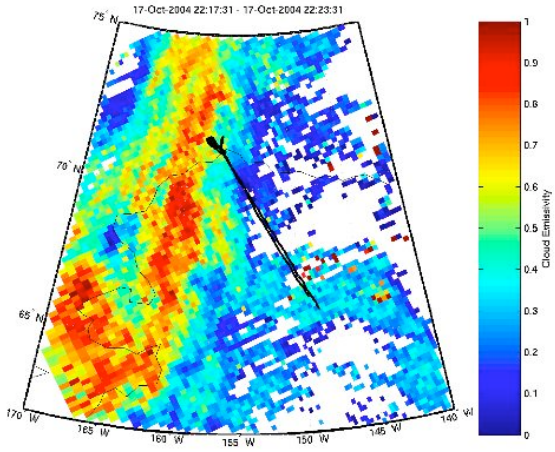

Figure 20: The AIRS cloud emissivity is presented using the Sorting/Slicing retrieval. The Proteus flight track is overlaid on the figure as the black line.

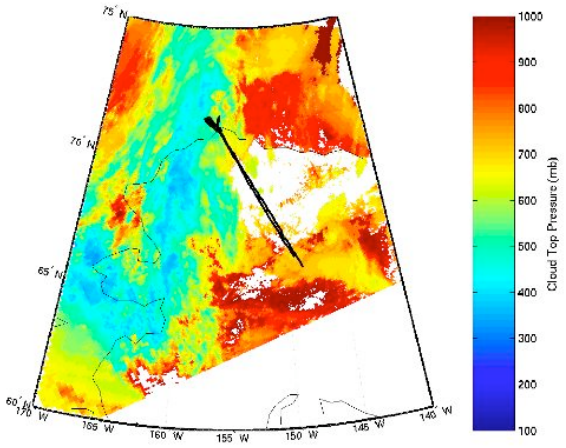

Figure 21: MODIS MYD06 cloud top height retrieval for the coincident MODIS granule on October 17th 2004 at 22:22 UTC. The CDL flight track is presented as the black line on the figure.

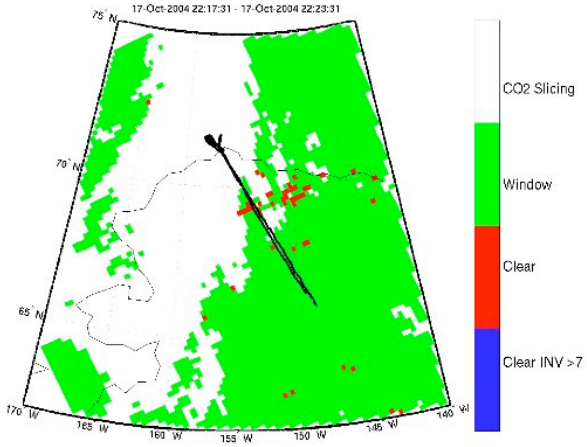

Figure 22: The cloud retrieval technique used in the optimal AIRS cloud top height in Figure 19. FOV that where determined clear are colored blue or red. The red pixels are determined clear using the spectral approach described in Chapter 0. The CO_2 Sorting/Slicing is presented as the white pixels in the figure. The green pixels are ones that the spectral test determined as low clouds and selected the Arctic window retrieval described Chapter 0.

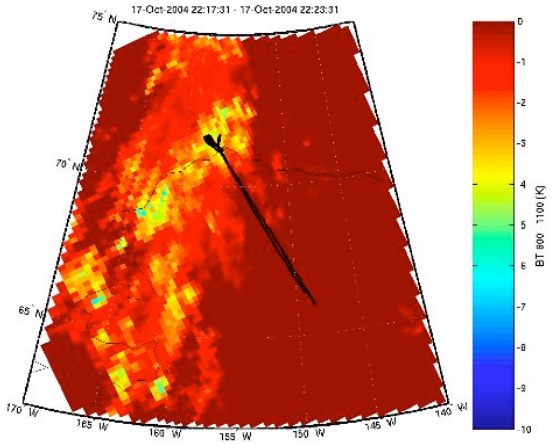

Figure 23: The AIRS BT800 – BT1100 channel differences for the NSA overpass at 22:22 UTC on October 17th 2004. BT800 – A BT1100 difference less then zero represent an ice signature and is used to select the Sorting/Slicing retrieval. The color scale has been set so that only FOV with the BT800 – BT1100 differences less then 0 has contrast. FOV with the BT differences greater then zero are red.

1.1.1 October 12th 2004

Low stratus covered the Arctic coast on October 12th with light snow falling from the cloud base at 0.6 km as presented in the AHSRL backscatter cross-section and depolarization measurements in Figure 24. The CDL backscatter profile for the Proteus flight is presented in Figure 25 with the flight track overlaid on Figure 26. The CDL measured cloud top height was 1.0 km during most of flight over the Arctic coast. The AHSRL measured low depolarization between 0.6 – 0.8 km with higher depolarization below 0.6 km confirming the cloud is composed of liquid water with ice falling from the bottom. The AIRS cloud top retrieval for the overpass at 22:05 UTC is presented in Figure 26.

The AIRS hyperspectral cloud retrieval correctly identifies the low stratus over NSA with a high 8-9 km ice cloud south of 68° N. The high clouds (7-9 km) cloud heights measured by the CDL at the beginning and end of the flight confirm the high cloud retrieved by AIRS in this region. The AIRS cloud mask in Figure 27 correctly selected the Sorting/Slicing retrieval for the high clouds and the Arctic window retrieval for the stratus over Barrow. The region centered at 68° N, -147 ° W in Figure 27 is determined clear by the AIRS cloud mask. The CDL detected clouds during the entire flight including the region identified as clear by AIRS. It is difficult to definitively determine the region was cloudy during the AIRS overpass as the Proteus flew over the area almost 2

hours after the overpass. The persistent low clouds measured by the CDL during flight suggest that this region could be misidentified as clear by the cloud mask.

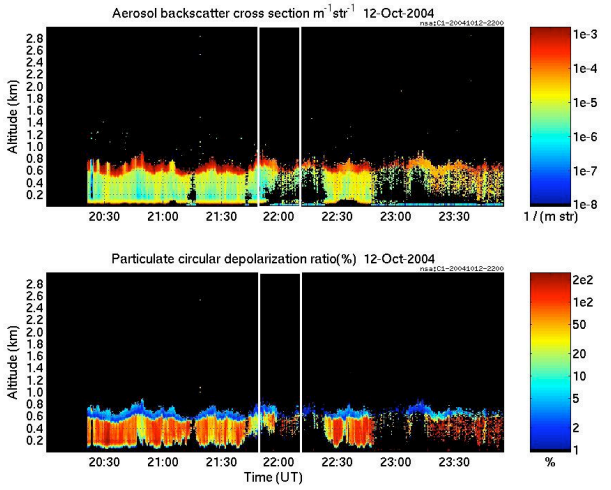

Figure 24: The AHSRL backscatter cross-section and depolarization from October 12th 2004. The AIRS overpass is occurred at the time marked by the white box. On this day the AHSRL laser power was low resulting in a reduced signal to noise.

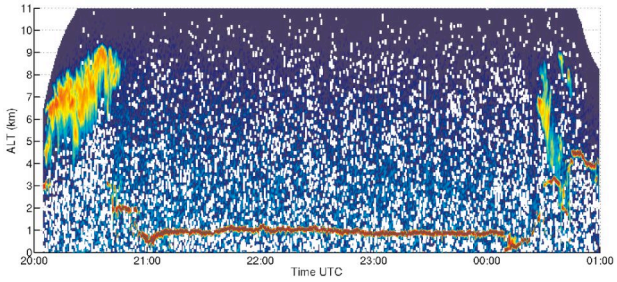

Figure 25: The Proteus CDL lidar backscatter profile for October 12th 2004. The flight track is presented in as the black line on Figure 26. The CDL detects a low status cloud with the cloud top at approximately 1.0 km between 21:00 – 00:00 UTC. The lidar is not able to penetrate to the surface indicative of a cloud optical thickness greater then 2.0.

The AIRS Arctic window retrieval over the NSA site retrieved a cloud height of 2.1 km compared to the CDL 1.0 km cloud top near the time of the AIRS overpass at 22:00 UTC. The Arctic window cloud top retrieval uses the AIRS inversion detection to determine if the cloud is above or below the inversion top. The NSA radiosonde and ECMWF temperature profile is presented in Figure 29. The profile has a weak inversion near the cloud top at 1.1 km that is resolved in the ECMWF profile. AIRS did not detect this inversion in Figure 28. If an inversion is not detected the AIRS retrieval matches the AIRS 11μm window BT to the ECMWF profile above the inversion top. AIRS did not detect the inversion and incorrectly matched the window BT above the inversion top at 2.1 km. The inversion strength measured by the radiosonde was approximately 3 K, close to the lower limit of the AIRS inversion sensitivity. The cloud optical depth estimated using the AHSRL was approximately 4.0, an optically thick cloud. To investigate the AIRS inversion sensitivity LBLDIS simulations where computed using the NSA radiosonde profile, CDL lidar cloud top and the estimated AHSRL cloud optical depth. The simulations in Figure 30 confirm AIRS does not have the sensitivity to resolve the inversion above this cloud. This illustrates a limitation of the AIRS Arctic window retrieval. For clouds below weak inversions the AIRS retrieval will overestimate the cloud top. This uncertainty is related to the depth and strength of the inversion above the cloud. Fortunately as the vertical depth and strength of the inversion increases the ability for AIRS to detect the inversion also increases which should limit the magnitude of the error on the height retrieval.

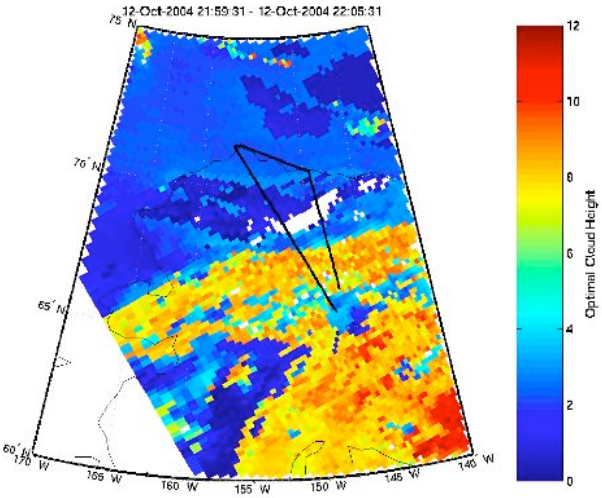

Figure 26: The AIRS optimal cloud height retrieval for October 12th 2004 granule #220. The Proteus flight track is presented as the black line on the figure.

The MODIS coincident cloud top pressure retrieval is presented in Figure 31. Both MODIS and AIRS detect cirrus south of Barrow and low stratus covering the Arctic coast. The MODIS retrieved cloud top height over the NSA facility was 2.0 km compared to the AIRS 2.1 km retrieval with both overestimating the cloud top by 1.0 km. The weak inversion above the cloud resulted in the AIRS retrieval incorrectly matching the profile above the inversion resulting in 1.0 km overestimate. The

MODIS cloud retrieval contains unphysical artifacts that appear as stripes over NSA and the Arctic Ocean in Figure 31. This error results from the NCEP atmospheric profile 1-degree spatial resolution. Both retrievals detect the high cirrus south of Barrow however the MODIS CO_2 slicing retrieval has more cloud height variability compared to the AIRS in Figure 26. It is not clear if the increased this results from the higher spatial resolution of MODIS or sensitivity to the cloud emissivity.

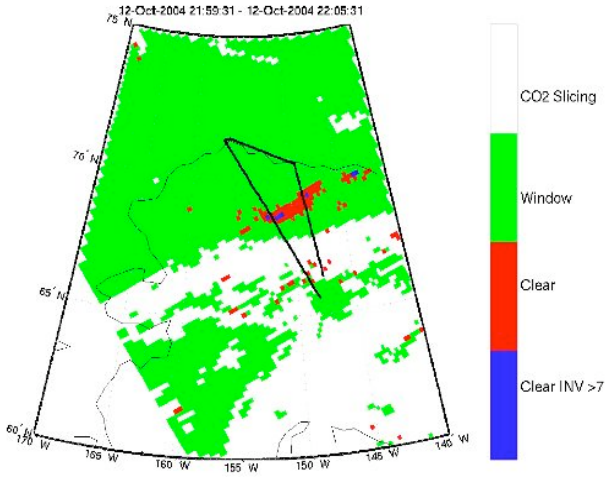

Figure 27: The AIRS cloud mask for October 12th 2004 is presented. The black line represents the Proteus flight track on this day.

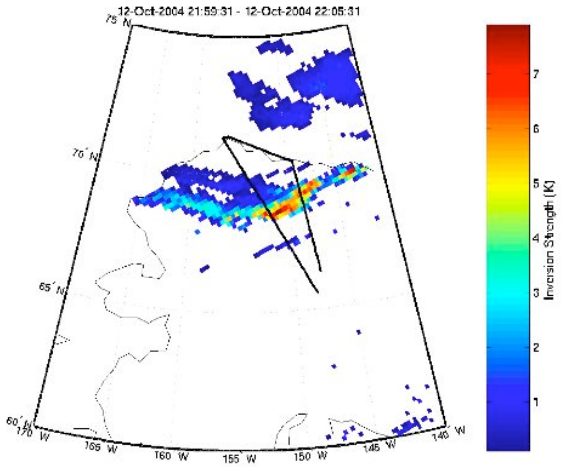

Figure 28: The measured inversion strength for October 12th 2004 is presented. White regions on the figure represent AIRS FOV where an inversion was not detected.

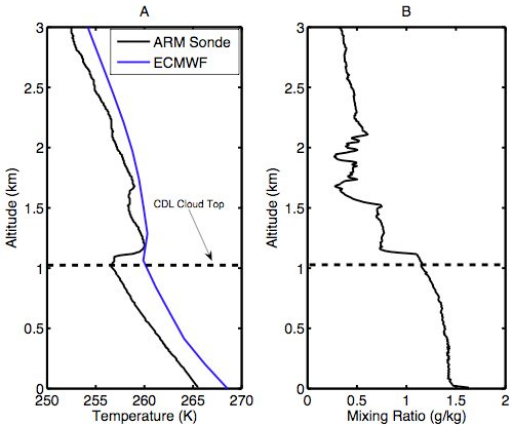

Figure 29: The NSA radiosonde profile launched at 22:00 UTC and the ECMWF temperature profile used in the AIRS retrieval over the NSA site is presented. The CDL cloud top over the NSA site at 21:45 is presented as the dashed line in the figure.

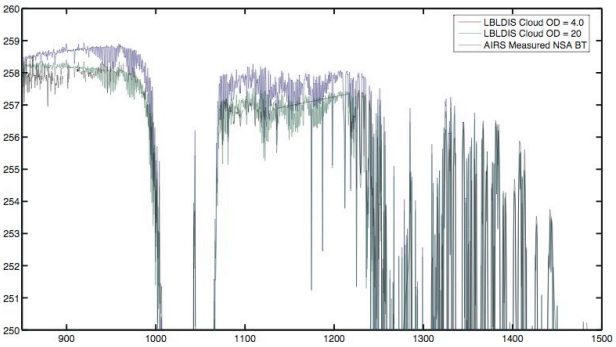

Figure 30: LBLDIS simulated BT spectra using the ARM NSA radiosonde, lidar cloud boundaries, and the AHSRL optical depth of 4.0. The AIRS PCA filtered BT spectra for the FOV over NSA is presented in black.

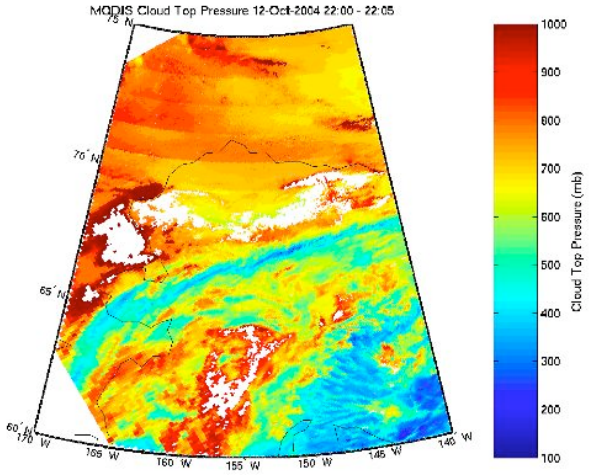

Figure 31: The MODIS cloud top pressure retrieval for October 12th 2004 at 22:00 UTC.

Winter AIRS Retrievals Over Barrow

The MPACE field experiment provided comprehensive validation with both ground and aircraft measurements. The experiment was conducted in October, a transitional period in the Arctic as the surface and cloud conditions are rapidly changing as the land and Arctic Ocean freeze. It is also the period with the highest cloud amounts (Curry et al., 1993). This section will focus on the winter months of January to March when the Arctic Ocean is completely frozen and no there is no solar contribution. Case studies for selected AIRS granules are compared to the ARM NSA surface measurements and MODIS. In this chapter the 150 AIRS and MODIS FOV over the Barrow NSA facility are compared to the NSA lidar-radar ARCL cloud top height retrieval over three-month period.

1.1.2 February 1st 2005

On this day a weather system over the Arctic Ocean is moving across the Barrow NSA site providing an interesting validation for the Arctic window cloud top retrieval discussed in Chapter 0 as the there are both low (1 km) and midlevel (3-4 km) clouds detected by the MPL lidar in Figure 6. There is a steep temperature inversion near the cloud top measured by the NSA radiosonde at 23:00 UTC in Figure 7. Two AIRS granules will be investigated. The first granule, at 13:00 UTC, a cloud with a 0.6 km cloud top is over the Barrow NSA site. A higher, 2.5 km cloud has just passed over the site at 22:00 UTC at the time of the second granule as determined by the MPL in Figure 6.

The AIRS measured window (900 cm^{-1}) BT for the 14:00 UTC AIRS granule is presented in Figure 34. The warmest brightness temperatures are north of the Arctic coast with the coldest temperatures in the interior of Alaska. The AIRS measured inversion strengths is presented in Figure 32 for the 14:00 UTC granule. A strong inversion is detected in the interior of Alaska, the location of the coldest window BT in Figure 34. North of the Arctic coast an inversion is not detected along the 73° N latitude line. A weaker inversion is detected north of 75° N between -170° W and -130° W, the location of the warmest measured window BT in Figure 34. In a standard atmosphere cold window BT typically represent cloudy regions. In the Arctic this is often not the case as the surface temperature is colder then atmosphere above. Strong inversions (> 15 degrees) occur primarily during clear sky conditions. The strong inversion detected in the interior of Alaska in Figure 32 is indicative of clear sky. Over Barrow the window BT is warmer with a BT of 244 K and measured inversion strength of 1.6 K. The NSA MPL detected a cloud at 0.6 km at the time of the overpass indicating that the inversion exists above the cloud.

The AIRS BT960 – BT1100 channel difference is presented in Figure 33. The BT960 – BT1100 difference is used by the Arctic cloud mask as one of the tests used to determine if a FOV is cloud filled. For BT differences greater then 1.0 K the FOV is determined cloudy in the cloud mask. The differences in Figure 33 have values larger then 1.0 in a large area north of Barrow. South of Barrow the BT differences are near zero, the same region as strongest inversions. The cloud mask for this granule using the thresholds described in Table 1 is presented in Figure 36. The red and blue regions are clear while the white and green regions are determined cloudy. If an ice cloud is detected using the BT800 – BT1100 channel differences the Sorting/Slicing retrieval is used and the FOV is colored white in the figure. If a water cloud is detected using the spectral test the Arctic window cloud height retrieval is used and labeled green in Figure 36.

The results from the AIRS cloud mask in Figure 36 detect low clouds over a large region of north of Barrow over the Arctic Ocean. The cloud mask did not detect clouds over much of the interior of Alaska. Over Barrow the cloud mask detected a low cloud agreeing with the MPL retrieved cloud height at 0.6 km. Figure 37 presents the optimal cloud top heights using the retrieval selected by the cloud mask (CO_2 Sorting/Slicing or the Arctic Window retrieval). The retrieval correctly identifies the low cloud over barrow with a cloud height of 0.1 km compared to the 0.6 km cloud height measured by the MPL. The AIRS retrieval detected a higher cloud just north of Barrow with cloud tops between 2 -3 km. Higher cloud top heights are retrieved where the AIRS inversion detection did not retrieve an inversion as the algorithm matches the window BT to the profile above the

inversion top for these cases. Over Barrow a weak inversion is detected resulting in the Arctic window retrieval correctly matching the window BT to the profile below the inversion top.

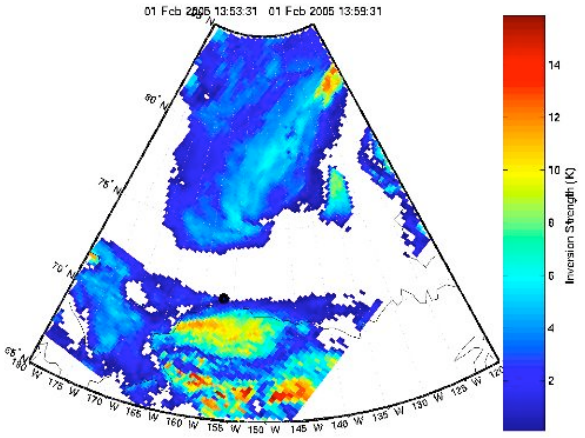

Figure 32: The AIRS retrieved inversion strength on February 1st 2005 at 14:00 UTC. The Barrow NSA site is marked by the black dot on the figure.

The MPL backscatter profile has low clouds (<1.0 km) over the NSA site at the 14:00 UTC AIRS overpass with a higher cloud layer moving in soon after in Figure 6. The AIRS overpass at 22:00 UTC occurs shortly after the higher 2.5 km cloud moves over the NSA site and is replaced by a 1.0 km cloud top height as measured by the MPL in Figure 6. The measured inversion strength for the 22:00 UTC AIRS granule is presented in Figure 35. The regions north of barrow where inversion was detected in Figure 32 has now move over the Barrow NSA and is located just south of Barrow. The lack of an inversion signal likely result from the higher 2.5 km cloud dominating the emission measured by the AIRS window channel and blocking the inversion signal. Using the inversion detection the Arctic window retrieval in Figure 38 resolves the higher cloud that transitioned over Barrow. The AIRS inversion retrieval detected an inversion strength of 2.7 K over Barrow resulting in the Arctic Window cloud top retrieval correctly matching the window BT to the temperature profile below inversion top and retrieving a cloud top height of 0.9 km.

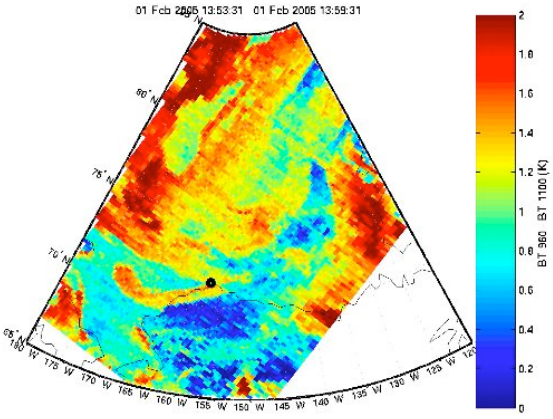

Figure 33: The AIRS BT960 – BT1100 channel BT differences for the February 1st 2005 14:00 UTC granule. The Barrow NSA site is marked by the black dot.

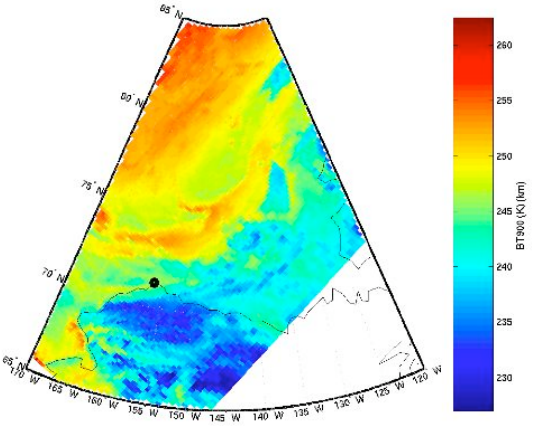

Figure 34: AIRS 900 (11μm) wavenumber BT on February 1st 2005 at 14:00 UTC. The Barrow NSA site is located at the black dot on the figure.

The AIRS Arctic cloud top retrieval successfully resolved the cloud height variations on February 1st 2005 using the retrieved inversion information. It would difficult to resolve the cloud variability on February 1st without the inversion information using just the window BT as there are two level in the atmospheric temperature profile that have temperatures at the measured cloud top temperature. To investigate if the AIRS Arctic cloud top retrieval is improving the cloud height results comparisons with the MODIS cloud top pressure retrieval for the coincident times is presented in Figure 38 and Figure 39. The AIRS and MODIS cloud top pressure for both the 14:00 and 22:00 UTC granules is presented in these figures. The AIRS 14:00 and 22:00 UTC granules resolve a 650 -750 mb cloud move over the NSA site

with a lower 900 mb cloud over the Arctic Ocean. This is in agreement with the MPL backscatter profile in Figure 6. Comparisons with the MODIS cloud heights in Figure 39 reveal that MODIS incorrectly inverts the cloud top pressures compared to the MPL. The temperature inversion results in the 2 -3 km cloud that passes over Barrow having warmer cloud top temperature then the lower 1.0 km cloud. Without the additional inversion information the MODIS retrieval cannot determine if the cloud is above or below the temperature inversion and incorrectly matches the warmer BT under the inversion top. The AIRS Arctic cloud top retrieval was able to resolve the 2.5 km cloud move over Barrow by using the AIRS inversion information.

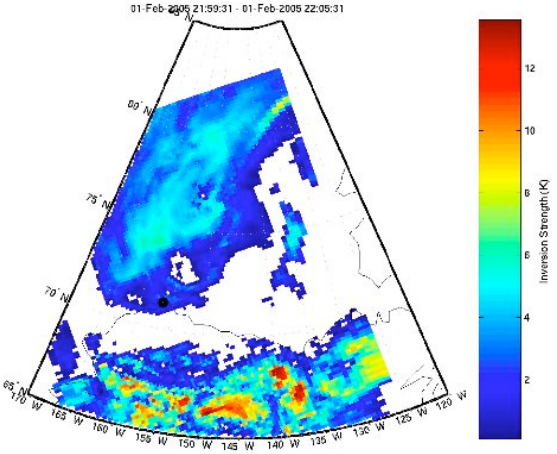

Figure 35: The measured AIRS inversion strength for the 22:00 UTC Barrow NSA overpass on February 1st 2005. The white regions on the figure are FOV where an inversion was not detected.

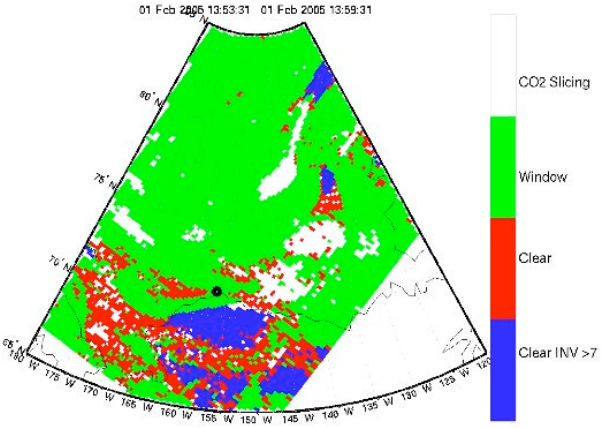

Figure 36: The AIRS Arctic cloud mask on February 1st 2005 at 14:00 UTC. FOV deterimiend clear using the inversion the inversion strength are colored blue. FOV deterimend clear using the spectral tests are red. Cloud FOV are colored green or white depending on the selected retrieval tequnque.

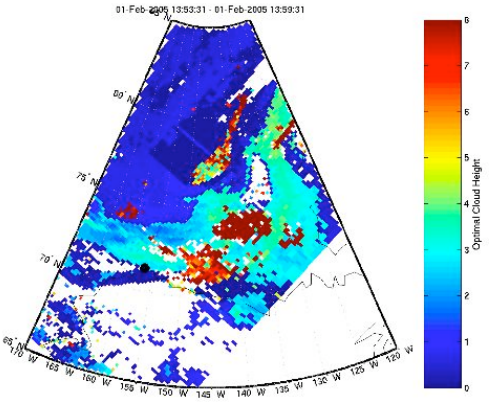

Figure 37: The AIRS optimal cloud height retrieval on February 1st 2005 at 14:00 UTC. FOV determined clear are white in the figure. The Barrow NSA site is marked by a black dot.

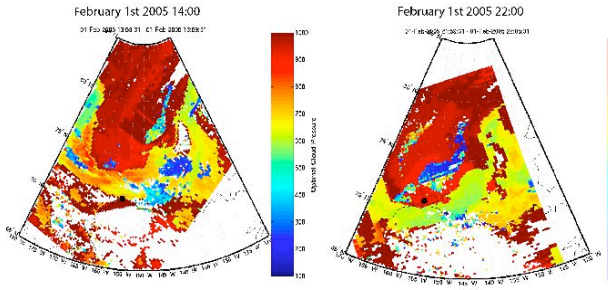

Figure 38: The AIRS Optimal cloud top pressure for the NSA overpass at 22:00 UTC on February 1st 2005. The clear regions are white in the figure.

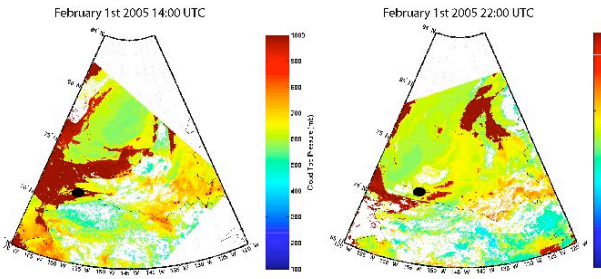

Figure 39: The MODIS cloud top pressure retrieval for the AIRS coincident 14:00 and 22:00 UTC granules in Figure 38 on February 1st 2005.

Three Months of AIRS Retrievals Over NSA

To investigate the accuracy of the AIRS Arctic cloud top retrievals 150 AIRS FOV over the ARM NSA site where selected for January, February, and October of 2004 and January and February of 2005. The AIRS cloud top heights for the FOV over NSA are compared to ARSCL lidar/radar cloud top retrieval and the coincident MODIS retrieval in this section.

Validation of a satellite measurements using ground-based instrumentation is a challenging endeavor. The AIRS nadir FOV has a surface footprint of 13 km compared to the up looking NSA radar and lidar FOV of only a few meters. The NSA is located a few hundred meters from the Arctic coast. This results in the AIRS FOV measuring both land and ocean emission. The coastal boundary can also effect the cloud concentration and microphysics resulting in additional biases. The higher spatial resolution of MODIS (5 km) reduces the sampling issues but even at the higher spatial resolution a MODIS FOV will have both land and ocean emission convolved in radiances. Cloud top retrievals using ground measurements have an inherent disadvantage as the cloud they have to penetrate through lower atmosphere and the cloud layers to retrieve a representative satellite cloud top height. The MPL at Barrow has a maximum optical depth sensitivity of approximately 2.5. The lidar sensitivity is less for high clouds as the signal measured by the lidar decrease by R^2 where R is the distance from the lidar. The MMCR radar does not have the attenuation problems however the MMCR is very sensitive to the size of the cloud particles. The backscatter intensity measured by the MMCR is dependent on the particle size with an R^6 dependence where R is particle maximum dimension. This results in the MMCR having reduced sensitivity to clouds with small particles. Cirrus clouds often have the smallest crystals concentrated near the top of the cloud resulting in the MMCR underestimating the cloud top.

Despite these difficulties if the limitations are understood the comparison can provide a unique understanding of the sensitivities of the satellite retrievals. To reduce the biases resulting from the AIRS 13 km surface footprint the ARCL cloud heights where averaged for a 30 minute period centered at the time of the AIRS overpass. If less then 25 % of the ARCL observations are clear the mean cloud top height of the cloudy ARCL measurements are recorded as the ARCL cloud height. If the ARCL determines clear sky for over 75% of the measurements the cloud conditions are recorded as clear. Using this method comparison to both the AIRS and MODIS cloud top height retrievals are made. The MODIS cloud height retrieval is recorded as an atmospheric pressure level. For this comparison the MODIS cloud pressure in converted into a cloud height using the ECMWF profile over Barrow so that it can be compared directly to ARCL.

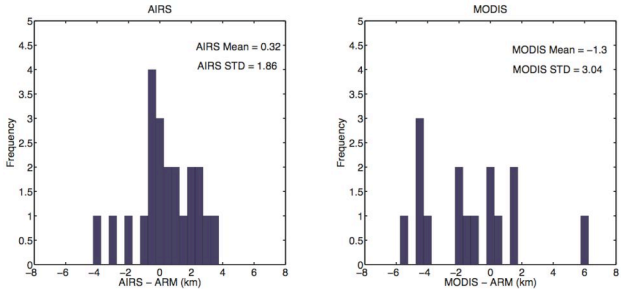

Figure 40:The Distribution of the difference between the retrieved cloud height for AIRS and MODIS compared to ARCL of FOV when ARCL retrieved a cloud height of greater then 4.0 km.

The AIRS retrieval used in this section where processed using an earlier version of the hyperspectral AIRS cloud mask that did not use the BT960 – BT1100 channel difference. Unfortunately access to the cluster computer system was limited and it was not possible to reprocess the 150 AIRS granules. It is expected that the addition of the BT960 – BT1100 channel should improve the cloud determination of clear and cloudy but have limited impact on the retrieved cloud heights.

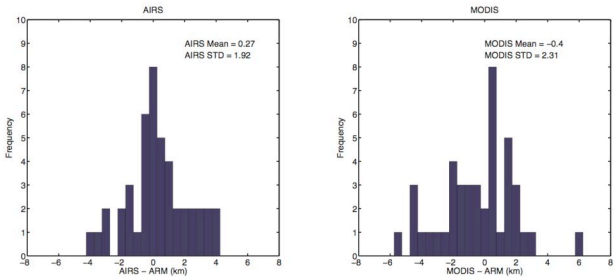

Figure 41: The difference between the retrieved cloud height for AIRS and MODIS compared to the Barrow NSA ARCL cloud top retrieval. A negative difference results if the AIRS or MODIS retrieved a cloud height lower then the ARCL. The distributions for MODIS include FOV where the instrument and ARCL detected the cloud.

The distribution of the differences between the AIRS optimal cloud top retrieval and the retrieved ARCL cloud height for the FOV determined cloud by AIRS and ARCL is presented in Figure 41. A positive difference results if AIRS detected a cloud above ARCL in the distribution. The MODIS distribution is calculated using the same method. Differences between the AIRS and MODIS cloud masks result in different compared to ARCL in the distributions. For example if AIRS and ACRL detected a cloud during an Aqua overpass but MODIS did not the AIRS distribution will include this overpass in the distribution while it will not be included in the MODIS as MODIS did not detect a cloud. In Figure 41 the differences between AIRS and the ARCL retrieval are smaller then MODIS with a standard deviation of 1.92 km compared to 2.31 km for MODIS. The AIRS retrieval tends to retrieve a cloud above ARCL with a mean 0.27 km. The peak of the distribution is centered at zero but there are significantly more retrievals that are higher then ARCL. MODIS tends to retrieve a cloud height below ARCL with a mean of -0.4 km. Figure 42 presents a similar distribution but in this figure only FOV where AIRS, MODIS, and ARCL detected a cloud during the Aqua overpass are included in the distribution. There is not a significant difference compared the distribution in Figure 41.

To investigate the accuracy of the AIRS and MODIS retrievals for high clouds (above 4.0 km) the data was filtered so that only FOV where the ARCL detected a cloud above 4.0 km where included. The filtered distribution is presented in Figure 40. Despite the lower spatial resolution of AIRS the AIRS retrieval significantly improves the cloud height results compared to MODIS. The mean and standard deviation of AIRS is similar to that of the complete data set with a mean of 0.32 km and a standard deviation of 1.86 km while MODIS demonstrates considerably less skill and significantly underestimates the cloud top height with a mean of -1.3 km and standard deviation of 3.04 km in Figure 40.

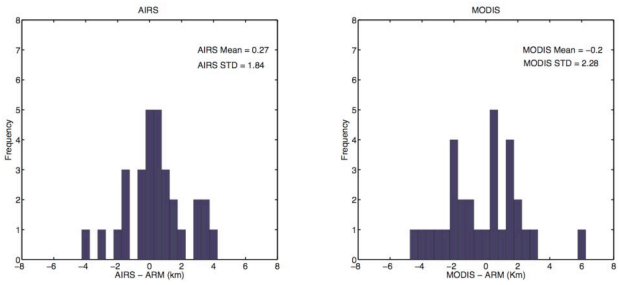

Figure 42: The Distribution of the difference between the retrieved cloud height for AIRS and MODIS compared to ARCL. In this distribution only AIRS and MODIS FOV where MODIS, AIRS, and ARCL detected a cloud are presented.

The AIRS cloud top height improvement for high clouds results from a combination of possible improvements. The hyperspectral CO_2 Sorting/Slicing retrieval likely contributes to the improvement based on the lidar comparisons presented in this paper. The AIRS cloud mask detected significantly more of the high clouds

compared to MODIS with AIRS detecting 70% of the cases when ARCL detected a cloud above 4 km compared to 48% of the cases for MODIS. An improved cloud retrieval selection algorithm will significantly improve the cloud top heights. If the 11 μm window retrieval is applied to optically thin cirrus significant errors will result. The AIRS retrieval developed in this paper uses a very different methodology to select the retrieval method compared to MODIS. The AIRS retrieval selects the retrieval based on spectral tests sensitive to cirrus. If cirrus are detected the CO_2 Sorting/Slicing retrieval is used. The MODIS retrieval first applies the CO_2 slicing retrieval to all FOV retrieved as cloudy by the MODIS cloud mask. If MODIS retrieval determines the quality of the CO_2 slicing retrieval insufficient it reverts to the 11 μm window retrieval resulting in the MODIS cloud height dependence on the methods used by MODIS to determine the quality of the CO_2 Slicing retrieval.

Figure 43 presents the AIRS and MODIS comparison to ARCL for FOV when ARCL detected clouds lower then 4.0 km. The AIRS distribution has two peaks, one centered near zero and the second at 3 km above ARCL. The MODIS distribution peaks at 1.0 km above ARCL without the second mode found in the AIRS results. This result was surprising as it was expected that the AIRS Arctic window retrieval would reduce the over estimation of the cloud heights using the added inversion information. To investigate these differences the granule day and time of the FOV with differences greater then 2.5 km where selected from the data set. The cloud heights for the three retrievals are listed in Table 2. AIRS retrieved the cloud height 4.1 km over the ARCL retrieval on the 13th of January 2004 while MODIS did not detect a cloud for this FOV. Inspection of the MPL backscatter profile reveals that there was a thin broken ice cloud between 4 -5 km that the ARCL retrieval did not detect. Typically the infrared retrievals will be less sensitive to optically thin clouds when compared to ARCL. On this day AIRS correctly retrieved the cloud height at 4.7 km using the CO_2 Sorting/Slicing retrieval. On February 17th ARCL detected the cloud at 1.5 km compared to 5.3 km and 4.3 km for AIRS and MODIS. Inspection of the MPL backscatter finds a very thin ice cloud between 0 – 3.5 km at the time of the overpass. The AIRS FOV correctly identified the cloud as ice and applied the CO_2 Sorting/Slicing retrieval. However the retrieval over estimated the cloud height by about 2 km.

The large AIRS retrieval differences compared to ARCL result from combination of errors in both the ARCL and AIRS retrieval. For all these cases the AIRS cloud height retrieval used the CO_2 Sorting/Slicing, not the Arctic window retrieval. In at least two of these cases after examination of the MPL backscatter the AIRS retrieval correctly retrieved the cloud height. For the other cases the MPL was attenuated and the actual cloud height could not be determined. This investigation highlights the importance understanding the limitations of the measurements. Large differences between ARCL and the satellite retrievals can result from both errors in the satellite and the ARCL retrieval. After removing the FOV with ARCL cloud top height errors the AIRS demonstrates a close comparison to ARCL.

Table 2: Cloud height results for days with AIRS –ARCL differences greater then 2.5 km

FOV Time	AIRS CLH	MODIS CLH	ARCL CLH	MPL Analysis
01-Jan-2003 13:20	4.5 km	2.3 km	0.9 km	MPL attenuated at 0.9 km
02-Jan-2003 14:03	3.4 km	2.7 km	0.6 km	Cloud at 3.0 km attenuated
13-Jan-2004 14:52	4.7 km	No cloud	0.6 km	Thin cirrus at 4–5 km
17-Feb-2004 15:23	5.3 km	4.3 km	1.5 km	Thin ice 0 - 3.5 km

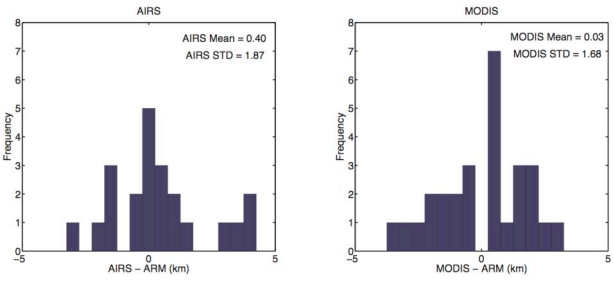

Figure 43: The Distribution of differences between the retrieved cloud height for AIRS and MODIS compared to ARCL when ARCL detected a cloud height less then 4.0 km.

Summary and Future Work

The goal of this paper was to improve the Arctic winter cloud climatology by utilizing the newly available satellite hyperspectral measurements. Using these measurements new retrieval techniques, designed specifically for the hyperspectral, were developed to improve the cloud top height retrievals of winter Arctic clouds. These new retrievals algorithms were rigorously validated using both collocated aircraft and ground

measurements. It is demonstrated that these new retrievals can significantly improve the satellite cloud top retrievals in the Arctic.

The retrievals developed in this paper are:

•A hyperspectral inversion detection retrieval that can definitively determine the presence of an inversion

•An Arctic cloud top retrieval that uses the inversion detection to improve the retrieved cloud top altitude for Arctic stratus clouds

The AIRS Arctic cloud top retrieval was compared to the coincident MODIS and the ground based ARCL lidar-radar at the ARM NSA research facility over a three-month period. In this comparison the ARCL retrieval is considered to be most sensitive to optically thin clouds as it uses the active remote sensed lidar cloud retrievals. Filtering the results so that only clouds above 4.0 km as determined by ARCL were considered, it is demonstrated that the AIRS CO_2 Sorting/Slicing cloud top retrieval had significantly smaller ARCL cloud height biases compared to the narrow band MODIS retrievals.

The hyperspectral inversion detection retrieval allows for definitive inversion detection in the AIRS FOV. This is a significant improvement compared to narrow band retrieval that require channel difference thresholds that are dependent on the strength and depth of the inversion. It is demonstrated that the hyperspectral inversion detection algorithm is significantly more sensitive to weak or shallow inversions with inversion sensitivity of approximately 3.0 K. The sensitivity is dependent on the vertical depth of the inversion and the atmospheric water vapor concentration.

An important finding from this paper is that the hyperspectral inversion retrieval detects temperature inversions above Arctic stratus. This has important implications as the presence of an inversion is often used in Arctic cloud masks to identify clear FOV. This finding suggests that for hyperspectral measurements this cloud mask technique will incorrectly identify cloudy FOV as clear. For the 150 AIRS FOV investigated in this paper the measured inversion strength was less 10.0 K when a cloud was present. Based on this observation for measured inversion strengths greater then 10.0 K there is a high probability that FOV is clear. For measured inversion strengths less then 10.0 K additional information is needed to determine if the FOV is clear or cloudy.

The frequent temperature inversion in the Arctic winter presents a challenge for infrared remote sensing of the cloud top as there are often multiple cloud top altitudes for a measured window BT (Key and Barry, 1989). The Arctic window cloud retrieval developed as part of the paper research uses the cloudy inversion detection to determine a unique cloud height for these cases. This new retrieval is applied to winter AIRS measurements over NSA. Comparisons with the aircraft and ground lidar measurements demonstrate that the additional inversion information can improve the Arctic window cloud top height retrievals.

The sensitivity of the Arctic window retrieval is investigated using simulations and comparisons to the NSA and aircraft lidar measurements. The validation demonstrates that using the inversion information can significantly improve the retrieved cloud top height. However, if the inversion strength above the cloud is weak, the inversion may not be detected. Using simulations it is demonstrated for inversion strengths less then 2-3 K AIRS will not detect the inversion. The cloud optical thickness impacts the detection sensitivity. Optically thin clouds reduce the inversion signature as the cloud top is often near the coldest temperature in the profile. As part of the validation found cases where a weak inversion existed above the cloud that was not detected by the AIRS retrieval. For these cases the AIRS retrieval incorrectly selected the cloud above the inversion top when the cloud was below the inversion. The error in the retrieved cloud height for this case was approximately 1.0 km.

The Arctic hyperspectral window retrieval requires a temperature profile that resolves the inversion in the profile. The AIRS retrievals presented in this paper used the ECMWF grid temperature profiles. For the cases investigated in this paper the ECMWF profiles did resolve inversions in the winter Arctic. The accuracy of the cloud top retrieval is dependent on the accuracy of the profile. Uncertainties in the profile contribute to the cloud height errors.

The CO_2 Sorting/Slicing and the Arctic window retrievals were combined into an optimal cloud height retrieval. As part of this research a new Arctic hyperspectral cloud mask was developed that uses the spectral differences between the surface and clouds. This cloud mask differs from the MODIS cloud mask that uses channels sensitive to the inversion to determine clear from cloudy. The new cloud mask was developed based on the finding in this paper that there is little correlation between cloudy or clear FOV and the detected inversion in the hyperspectral measurements. Spectral tests, sensitive to phase, are used to select the optimal cloud height retrieval (CO_2 Sorting/Slicing or the Arctic window retrieval).

Comparisons between the AIRS optimal cloud top height retrieval, MODIS, and the NSA ARCL were investigated for 150 AIRS/MODIS FOV for three months of winter NSA overpasses. It is found that the AIRS hyperspectral cloud top retrieval improved the cloud heights compared to the MODIS retrieval. For the 150 FOV MODIS had a mean difference of -0.40 km with a standard deviation of 2.31 km compared to the AIRS mean difference of 0.27 km with a standard deviation of 1.92 km. If both retrievals had identical performance, MODIS, with its higher spatial resolution, should compare closer to ARCL then AIRS. The smaller AIRS ARCL bias despite the resolution handicap is encouraging.

Future research plans include a more extensive validation using measurements from multiple locations in the Arctic. Arctic surface and cloud conditions demonstrate significant geographic variability. This variably may impact the cloud top height retrievals. The AHSRL has recently found a permanent home in northern Canada at the NOAA research facility on Ellesmere Island at latitude of 80° N. The data collected at Ellesmere this winter will provide a new validation data set with AHSRL high quality extinction profiles and depolarization measurements. This will allow for the investigation of the AIRS cloud height sensitivities to the cloud optical depth and phase.

Bibliography

Ackerman, S. A., 1996: Global Satellite Observations of Negative Brightness Temperature Differences between 11 and 6.7 um. *Journal of the Atmospheric Sciences*, **53,** 2803-2812.

Ackerman, S. A., W. L. Smith, H. E. Revercomb, and J. D. Spinhirne, 1990: The 27-28 October 1986 FIRE IFO Cirrus Case Study: Spectral Properties of Cirrus Clouds in the 8-12 mum Window. *Monthly Weather Review*, **118,** 2377-2388.

Aumann, H. H., M. T. Chahine, C. Gautier, M. D. Goldberg, L. M. Kalnay, L. M. McMillin, H. E. Revercomb, W. L. Rosenkranz, W. L. Smith, D. H. Staelin, L. L. Strow, and J. Susskind, 2003: AIRS/AMSU/HSB on the Aqua mission: Design, science objectives, data products, and processing systems. *IEEE Transactions on Geoscience and Remote Sensing*, **41,** 253-264.

Baum, B. A., P. F. Soulen, K. I. Strabala, M. D. King, S. A. Ackerman, W. P. Menzel, and P. Yang, 2000: Remote sensing of cloud properties using MODIS airborne simulator imagery during SUCCESS 2. Cloud thermodynamic phase. *Journal of Geophysical Research*, **105,** 11781-11792.

Curry, J. A., J. L. Schramm, and E. E. Ebert, 1993: Impact of Clouds on the Surface Radiation Balance of the Arctic-Ocean. *Meteorology and Atmospheric Physics*, **51,** 197-217.

Curry, J. A., W. B. Rossow, D. Randall, and J. L. Schramm, 1996: Overview of Arctic cloud and radiation characteristics. *Journal of Climate*, **9,** 1731-1764.

Key, J. and R. G. Barry, 1989: Cloud Cover Analysis with Arctic Avhrr Data.1. Cloud Detection. *Journal of Geophysical Research-Atmospheres*, **94,** 18521-18535.

Key, J., J. A. Maslanik, and A. J. Schweiger, 1989: Classification of Merged Avhrr and Smmr Arctic Data with Neural Networks. *Photogrammetric Engineering and Remote Sensing*, **55,** 1331-1338.

Key, J. R., A. J. Schweiger, and R. S. Stone, 1997: Expected uncertainty in satellite-derived estimates of the surface radiation budget at high latitudes. *Journal of Geophysical Research-Oceans*, **102,** 15837-15847.

Liu, Y. H. and J. R. Key, 2003: Detection and analysis of clear-sky, low-level atmospheric temperature inversions with MODIS. *Journal of Atmospheric and Oceanic Technology*, **20,** 1727-1737.

Liu, Y. H., J. Key, R. A. Frey, S. A. Ackerman, and W. P. Menzel, 2004: Night Time Polar Cloud Dectection with Modis. *Remote Sensing of the Environment*.

Mahesh, A., V. P. Walden, and S. G. Warren, 2001: Ground-Based Infrared Remote Sensing of Cloud Properties over the Antarctic Plateau. Part II: Cloud Optical Depths and Particle Sizes. *Journal of Applied Meteorology*, **40,** 1279-1294.

Strabala, K. I., S. A. Ackerman, and W. P. Menzel, 1994: Cloud Properties inferred from 8{#150}12-um Data. *Journal of Applied Meteorology*, **33,** 212-229.

Turner, D., 2003: Microphysical properties of single and mixed-phase arctic cluods derived from ground-based

AERI observations, Atmospheric and Oceanic Sciences,
University of Wisconsin, Madison, 181.